

## Hydrostatic pressure coefficients of the photoluminescence of $\text{In}_x\text{Ga}_{1-x}\text{As}/\text{GaAs}$ strained-layer quantum wells

V. A. Wilkinson,\* A. D. Prins,\* J. D. Lambkin, E. P. O'Reilly,\*  
D. J. Dunstan,\* and L. K. Howard

*Strained-Layer Structures Research Group, University of Surrey, Guildford, Surrey GU2 5XH, United Kingdom*

M. T. Emeny

*Royal Signals and Radar Establishment, Saint Andrew's Road, Malvern, Worcestershire WR14 3PS, United Kingdom*

(Received 20 February 1990)

The photoluminescence of strained  $\text{In}_x\text{Ga}_{1-x}\text{As}$  quantum wells, with  $x$  up to 0.225, grown pseudomorphically between unstrained GaAs barriers, has been studied under high hydrostatic pressure in a diamond-anvil cell. The measured direct-band-gap pressure coefficients show a marked deviation from theoretical predictions; they decrease strikingly below the GaAs value of 10.7 meV/kbar as the well width or the indium content is increased; the pressure coefficient of the band gap in wide wells depends on well composition  $x$  as  $10.7 - 6.0x$  meV/kbar in the samples studied, compared with a predicted variation of  $10.7 - 1.7x$  meV/kbar calculated with use of third-order elasticity theory. The experimental data could correspond to a composition dependence of the band-gap hydrostatic deformation potential,  $\alpha$ , of  $-7.99(1 - 0.47x)$  eV for small  $x$ . We speculate that the anomalously low measured pressure coefficients may be due to an interplay of effects related to disorder and strain in the alloy quantum wells.

### I. INTRODUCTION

There is increasing interest in the growth of strained-layer semiconductor structures for device applications.<sup>1-3</sup> The greatest effort to date has concentrated on the growth of  $\text{In}_x\text{Ga}_{1-x}\text{As}$  pseudomorphic layers on GaAs. Compared with the well-established GaAs/ $\text{Al}_x\text{Ga}_{1-x}\text{As}$  system, few of the fundamental parameters necessary for the engineering of  $\text{In}_x\text{Ga}_{1-x}\text{As}$ -based devices are yet known. Such parameters are particularly important as the built-in lattice mismatch causes both hydrostatic and axial deformation of the strained quantum wells. Some deformation potentials have been measured for InAs, and also for  $\text{In}_{0.53}\text{Ga}_{0.47}\text{As}$  lattice matched to InP, and these may be used to interpolate values for  $\text{In}_x\text{Ga}_{1-x}\text{As}$  strained layers on GaAs. Measurements of photoluminescence (PL) under high pressure can provide a direct determination of some of the important material parameters,<sup>4</sup> and in this paper we report new values for the hydrostatic pressure coefficients of  $\text{In}_x\text{Ga}_{1-x}\text{As}$  quantum wells between GaAs barriers, and for the corresponding band-gap deformation potentials. We find a striking decrease of the PL pressure coefficient with increasing indium concentration and with increasing well width. This decrease cannot be accounted for by theoretical models based on interpolated elastic constants and deformation potentials and, at present, lacks a firm explanation.

There is already evidence in the literature of low PL pressure coefficients in  $\text{In}_x\text{Ga}_{1-x}\text{As}$  quantum wells of a particular composition, with values decreasing with increasing well width. Wang *et al.*<sup>5</sup> reported on a sample

with  $x=0.25$ , and while they commented that the pressure coefficients were close to that of GaAs (10.7 meV/kbar), it is noticeable in their data that the alloy values are, in fact, significantly lower (e.g., 10.0 meV/kbar for a 22-Å well). We have briefly reported on two samples which show conclusively that the PL pressure coefficient decreases with increasing well width at a fixed composition.<sup>6</sup> By studying a sample with three wells of constant width but different compositions, we show in this paper that the PL pressure coefficient also decreases with increasing alloy composition and hence with strain. We compare the results with those from one of our previous samples and show that the results are consistent with the PL pressure coefficient,  $dE_g/dP$ , of the direct band gap of pseudomorphic  $\text{In}_x\text{Ga}_{1-x}\text{As}$  on GaAs varying with  $x$  as  $10.7 - 6.0x$  meV/kbar for the range of samples studied. This unexpectedly large variation in pressure coefficient with built-in axial strain has led us to examine the predicted strain dependence of the band gap, and, in particular, whether either the deformation potentials or elastic constants should be strongly strain dependent. Local-density calculations indicate that the band-gap deformation potential,  $\alpha$ , should show little variation with axial strain in the samples studied. We find that the inclusion of third-order elastic constants leads to a predicted pressure dependence of the band gap of  $10.7 - 1.7x$  meV/kbar, so that neither this effect nor the strain dependence of the deformation potentials are sufficient to explain the experimental data. The new experimental results are described in the next section, with the theoretical analysis and discussion following in Sec. III. Finally, we summarize our conclusions in Sec. IV.

## II. EXPERIMENTAL DETAILS AND RESULTS

The samples were grown by molecular-beam epitaxy in a Vacuum Generators V80H reactor at the Royal Signals and Radar Establishment. The substrate temperature was determined from the GaAs surface-reconstruction transition temperature,  $T_t$ , observed by reflection high-energy electron diffraction (RHEED), and the quantum wells were grown at a substrate temperature,  $T_t - 11$  K, already known not to give significant indium desorption under the growth conditions used in this reactor.<sup>7</sup> The Ga and In beam fluxes were set to give growth at about 1 monolayer/s, using RHEED oscillations to set the intensities of the two beams and hence the quantum-well composition,  $x$ . The compositions predicted from the RHEED oscillations were confirmed on a number of thick relaxed layers of  $\text{In}_x\text{Ga}_{1-x}\text{As}$  by several techniques (energy-dispersive x-ray microprobe, Rutherford backscattering, optical absorption, and double crystal x-ray diffraction) and were found to be accurate, in this range of composition, to about  $\pm 0.01$ . We note that the quantum-well compositions cannot be determined directly by these techniques because of the small quantity of material in the well, and that an exact determination of the composition from PL requires knowledge of a wide range of parameters, such as deformation potentials, alloy bowing, and confinement energies. Consequently, PL can only be used to detect gross errors of composition, in excess of about 1% or 10–20 meV in band gap. In our quantum wells, PL confirms that the compositions do not differ significantly from the compositions deduced from the RHEED oscillations, and so we take these as the actual compositions.

Sample A (“ME501”) was grown with four quantum wells of constant composition and different widths (see Table I). Sample B (“ME566”) contained three quantum wells of the same width, but different compositions. The well widths,  $L_z$ , were also chosen to be below both the critical thicknesses calculated by theory<sup>8</sup> and those found for these compositions and growth conditions by our own transmission-electron-microscopy (TEM) studies.<sup>9</sup> The GaAs barriers were 500 Å wide, so that each quantum well would be independent, both electronically and structurally, of its neighbors. The samples were nominally undoped, with a background  $n$ -type doping of about  $10^{14} \text{ cm}^{-3}$ .

For the high-pressure measurements the substrates

were thinned mechanically to a thickness of about 30  $\mu\text{m}$ , and the samples were cleaved to about  $100 \mu\text{m} \times 100 \mu\text{m}$  for loading, together with a piece of GaAs to serve as the pressure gauge, in the diamond-anvil cell (DAC).<sup>10</sup> In the case of sample B, a piece of InP was also loaded to serve as a pressure gauge above about 40 kbar, where the GaAs becomes indirect and its PL quenches. Argon was used as the pressure-transmitting fluid. PL spectra were obtained at 80 and 20 K, and pressure changes were made at the measurement temperature.

The PL spectrum of sample B at 5 kbar is shown in Fig. 1, where we see a sharp peak associated with each of the quantum wells, confirming the quality of the strained layers. Under pressure, all peaks shift to higher energy at about the same rate, with pressure coefficients close to the 10 meV/kbar value characteristic of direct  $\Gamma_6-\Gamma_8$  transitions in the tetrahedral semiconductors.<sup>11</sup> As the pressure was raised, each peak quenched in turn, with the emission of the GaAs pressure gauge disappearing first at about 40 kbar, and finally the emission from the deepest well at about 50 kbar. This limited the pressure range of the experiments. The quenching contains information about the electronic band structure of the  $\text{In}_x\text{Ga}_{1-x}\text{As}/\text{GaAs}$  heterostructures, but this will be presented elsewhere: in this paper we are concerned solely with the pressure coefficients.

The most precise values for the measured pressure coefficients are obtained by plotting the PL peak energies against the energy of an emission band whose pressure coefficient is already known,<sup>12</sup> and preferably a band which is of physical significance in the problem. Here we use the band-edge emission of GaAs, which increases at 10.7 meV/kbar,<sup>4</sup> until it quenches. Above the GaAs quenching pressure, we use InP, which moves at 8.5 meV/kbar to 0.018 meV/kbar.<sup>2,13</sup> The GaAs direct gap can then be estimated taking account of nonlinearity in the GaAs pressure coefficient ( $-0.014 \text{ meV/kbar}^2$ ),<sup>14</sup> which becomes significant at these pressures. The GaAs coefficient is of obvious physical significance in the  $\text{In}_x\text{Ga}_{1-x}\text{As}$  system, since it is the limiting material as  $x$

TABLE I. Sample parameters.

Sample	Well		Pressure coefficient (meV/kbar)
	$L_z$ (Å)	$x$	
A (“ME501”)	30	0.18	9.9
	40	0.18	9.8
	60	0.18	9.5
	120	0.18	9.4
B (“ME566”)	100	0.09	10.2
	100	0.15	9.8
	100	0.225	9.3

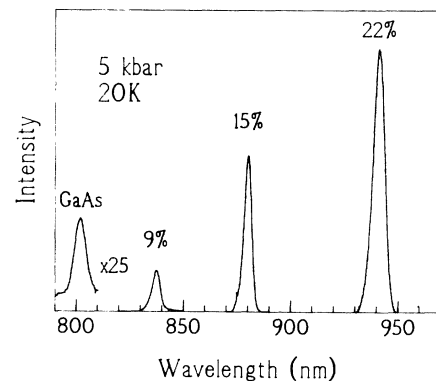


FIG. 1. Typical photoluminescence spectrum at high pressure, from sample B, with three 100-Å quantum wells of different compositions (Table I). The GaAs emission from the pressure gauge is also shown.

goes to 0. InP is used simply as a convenient pressure gauge. We plot in Fig. 2 the difference between the quantum-well and GaAs emission energies against the GaAs emission energy, for the sample with wells of constant width but varying composition (sample B). We see that the three quantum-well emission energies are moving at different rates, and that the PL pressure coefficients decrease with increasing In composition. The measured pressure coefficients are given in Table I.

We note that errors in the measured pressure are unimportant when the data are presented in this way. We are plotting in Fig. 2 the *difference* between the PL pressure coefficient of the GaAs band gap and the  $\text{In}_x\text{Ga}_{1-x}\text{As}$  quantum-well band gap, and so we are insensitive to errors in the absolute value of the GaAs pressure coefficient. The GaAs emission band is, however, weaker than the quantum-well emissions (Fig. 1), and so any error in the determination of its peak energy shows up as a scatter in the data with the same scatter for all the wells, as seen in Fig. 2. We also see in Fig. 2 a strong decrease in the pressure coefficient for each quantum well close to the quenching pressure. This is attributed to band mixing and will be discussed in detail elsewhere. The pressure coefficients reported here are fits to the linear sections of the data.

### III. ANALYSIS AND DISCUSSION

The pressure coefficient of the emission from a quantum well of a given composition  $x$  can vary with well

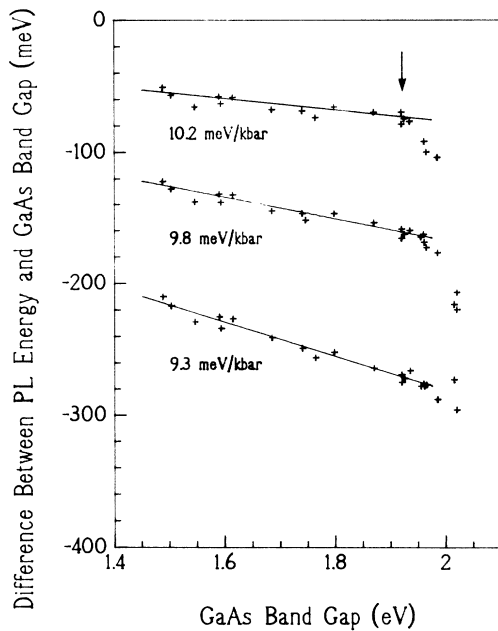


FIG. 2. Difference between the photoluminescence peak energies of the three quantum wells in sample B and the GaAs peak energy are plotted against the energy of the GaAs emission. Above the GaAs quenching energy, marked by the arrow, the GaAs values are extrapolations using the InP pressure gauge.

width,  $L_z$ , because of effects related to the confinement energy.<sup>15</sup> When the well is very wide, the confinement energy vanishes, the confined states behave exactly as the band edge in the bulk material, and the pressure coefficient is that of the equivalent bulk crystal. In this section, we first use our previous PL data<sup>6</sup> on the sample with  $\text{In}_{0.18}\text{Ga}_{0.82}\text{As}$  quantum wells of various thicknesses to deduce the pressure coefficient and deformation potential of the equivalent strained bulk material (the limit of a wide well). We confirm that the wide-well PL pressure coefficient is significantly lower than that of bulk GaAs. We then analyze the data from Fig. 2 and find that the pressure coefficient decreases linearly with increasing In content  $x$ , at least up to  $x=0.225$ . We seek to explain this behavior by considering the possibility of strain-dependent deformation potentials or of strain-dependent elastic constants. Our calculations indicate that these mechanisms are not sufficient to explain the experimental data and so we consider what further mechanisms may be occurring.

Figure 3 shows the measured pressure dependence of the quantum-well emission for sample A as a function of well width (solid circles), along with the calculated pressure dependence under various assumptions. We use a 60:40 (conduction band):(heavy-hole valence band) offset ratio at  $P=1$  bar in all of the calculations,<sup>16</sup> and assume that the electron effective mass,  $m_e^*$ , increases linearly with increasing band gap. When the well width  $L_z$  is very small, most of the confined-state wave function is in the GaAs barriers and therefore, as  $L_z \rightarrow 0$ , the pressure coefficient always approaches that of GaAs as in Fig. 3. For curve *a*, we assume that the pressure dependence of the quantum-well band gap equals that of GaAs, 10.7 meV/kbar, and that the band offsets do not vary with pressure. In this case, the pressure coefficient remains above 10.5 meV/kbar at all well widths, significantly

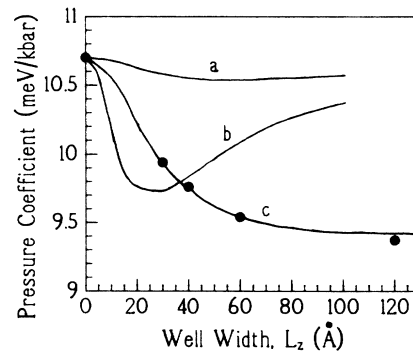


FIG. 3. Data points (solid circles) show the pressure coefficients of the various wells in sample A (for which  $x=0.18$ ) plotted against the well width,  $L_z$ . The solid curves, labeled *a*–*c*, show the calculated pressure coefficients as a function of  $L_z$ , using different assumptions described in the text for the pressure dependence of the quantum-well band gap and band offsets. The best agreement is obtained by assuming that the quantum-well band gap increases at 9.4 meV/kbar and that the valence-band offset is independent of pressure (curve *c*).

overestimating the experimental pressure coefficients. The small deviation below the value of 10.7 meV/kbar for wells of intermediate width is due to the pressure dependence of the electron effective mass, which leads to a reduction of the confinement energy with increasing pressure. In curve *b*, we show that it is not possible to get the required reduction in the pressure coefficient by varying the band-offset ratio with pressure while keeping the pressure dependence of the quantum-well band gap constant at 10.7 meV/kbar. We increase the heavy-hole band offset by 1.5 meV/kbar. We find that this can account reasonably well for the experimental data in the thinnest wells ( $L_z \lesssim 40$  Å), but, again, it significantly overestimates the pressure coefficients of the wider wells. Curves *a* and *b* establish that the pressure coefficient of the quantum-well band gap must be decreased compared to the GaAs value. We find that excellent agreement is obtained between theory and experiment when, in curve *c*, we assume that the wide-well pressure coefficient is 9.4 meV/kbar and that the magnitude of the valence-band offset is independent of pressure. We also note from curve *c* that the calculated pressure coefficient for a 100-Å quantum well is within 0.1 meV/kbar of the value for an equivalent bulk sample.

The variation of pressure coefficient with alloy composition is plotted in Fig. 4 for the wide-well limit, where we show the experimental coefficients for the 100-Å wells in sample B (solid circles), together with values from the literature for InAs (Ref. 17) and for bulk unstrained  $\text{In}_{0.53}\text{Ga}_{0.47}\text{As}$  lattice matched to InP (Ref. 18) (solid diamonds). The data indicate that the PL pressure coefficient in the quantum wells is reduced linearly from the GaAs value, and varies with alloy composition  $x$  as  $10.7 - 6.0x$  meV/kbar. In contrast, from the bulk values, the pressure coefficient would be expected to remain almost constant.

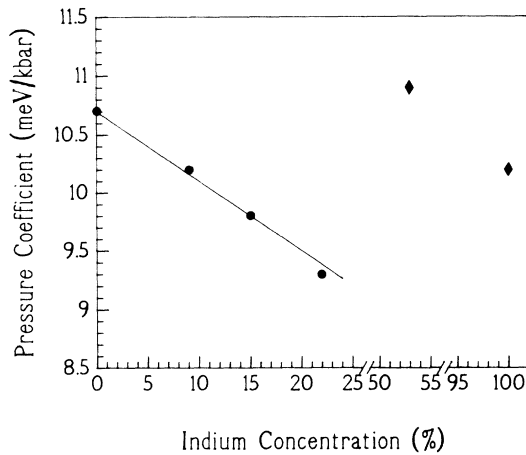


FIG. 4. Pressure coefficients of 100-Å quantum wells of  $\text{In}_x\text{Ga}_{1-x}\text{As}$  of various compositions are plotted against the compositions  $x$  (solid circles). The solid line is the linear fit,  $10.7 - 6.0x$  meV/kbar. Also shown for comparison are the measured pressure coefficients of  $\text{In}_{0.53}\text{Ga}_{0.47}\text{As}$  and InAs (solid diamonds).

This is a most surprising result. We have considered several possible explanations. None, as yet, can account quantitatively for the data. We have already seen from Fig. 3 that rapid variation of the band-offset ratio with pressure cannot explain the experimental results. We now turn to consider the influence of higher-order elastic constants and strain-dependent deformation potentials on the pressure coefficients.

For the structures we are considering, it is reasonable to assume that almost all the strain is incorporated in the quantum-well layers. Each well layer is under a biaxial stress such that its in-plane lattice constant,  $a_{\parallel}$ , equals the GaAs substrate lattice constant,  $a_s$ . The net strain in the well plane,  $\epsilon_{\parallel}$  is given by

$$\epsilon_{\parallel} = \epsilon_{xx} = \epsilon_{yy} = (a_s - a_x)/a_x, \quad (1)$$

where  $a_x$  is the lattice constant of the equivalent unstrained alloy. In response to the biaxial stress, the layer relaxes along the growth direction  $z$ , the strain  $\epsilon_{\perp}$  ( $=\epsilon_{zz}$ ) being of opposite sign to  $\epsilon_{\parallel}$  and given at  $P=0$  in second-order elasticity theory by

$$\epsilon_{\perp} = -\frac{2\sigma}{1-\sigma}\epsilon_{\parallel}, \quad (2)$$

where  $\sigma$  is Poisson's ratio. The total strain can be resolved into a purely axial component,  $\epsilon_{ax}$ , and a hydrostatic component,  $\epsilon_{vol}$ ,

$$\epsilon_{ax} = \epsilon_{\perp} - \epsilon_{\parallel}, \quad (3)$$

$$\begin{aligned} \epsilon_{vol} &= \epsilon_{xx} + \epsilon_{yy} + \epsilon_{zz} \\ &= 2\epsilon_{\parallel} + \epsilon_{\perp}. \end{aligned}$$

This built-in strain modifies the band gap  $E_g$  of the layer from its unstrained value,  $E_g^0$ , to

$$E_g = E_g^0 + \alpha\epsilon_{vol} - |\mathcal{L}\epsilon_{ax}|, \quad (4)$$

where  $\alpha$  is its hydrostatic band-gap deformation potential and  $\mathcal{L}$  its axial deformation potential, related to the splitting of the valence-band maximum induced by axial strain.<sup>3</sup> The bulk deformation potentials  $\alpha$  and  $\mathcal{L}$  are both negative quantities and, for a layer under biaxial compression, as here, Eq. (3) gives  $\epsilon_{ax} > 0$ . We can use (3) to rewrite (4) as

$$E_g = E_g^0 + 3\alpha\epsilon_{\parallel} + (\alpha + \mathcal{L})\epsilon_{ax}. \quad (5)$$

The band gap is then found to vary with pressure according to

$$\frac{dE_g}{dP} = \alpha \frac{d}{dP}(3\epsilon_{\parallel}) + (\alpha + \mathcal{L}) \frac{d\epsilon_{ax}}{dP}. \quad (6)$$

Equation (6) is a particularly useful way of writing the band-gap pressure coefficient of the alloy layer, as the in-plane lattice constant varies with pressure at the same rate as the GaAs lattice constant, so we can replace  $(d/dP)(3\epsilon_{\parallel})$  by  $-B_s^{-1}$ , where  $B_s$  is the GaAs bulk modulus. For a free-standing layer with the same indium content  $x$  as the strained layer, the band-gap pressure coefficient is given by

$$\frac{dE_g^0}{dP} = -\frac{\alpha}{B_x}, \quad (7)$$

where  $B_x$  is the bulk modulus of the free-standing alloy. We substitute (7) in (6) and, assuming for now that the deformation potentials are independent of strain, find the strained-well pressure coefficient in terms of the unstrained-alloy coefficient,

$$\frac{dE_g}{dP} = \frac{B_x}{B_s} \frac{dE_g^0}{dP} + (\alpha + \ell) \frac{d\varepsilon_{ax}}{dP}. \quad (8)$$

We can make reasonable estimates of all the terms on the right-hand side of (8) to predict the pressure dependence of the quantum-well band gap as a function of lattice mismatch.

We see in Fig. 4 that the pressure coefficients of GaAs,  $\text{In}_{0.53}\text{Ga}_{0.47}\text{As}$  on InP, and InAs bulk samples are 10.7, 10.95, and 10.2 meV/kbar, respectively, suggesting an approximately constant pressure coefficient across the complete alloy range, so we take  $dE_g^0(x)/dP = 10.7$  meV/kbar for the free-standing alloy with In content  $x$ . The bulk modulus  $B_x$  of  $\text{In}_x\text{Ga}_{1-x}\text{As}$  alloys of arbitrary composi-

tion has not been measured, but, for a wide range of III-V alloys,  $B$  has been observed to follow the empirical relation  $B \propto a^{-4}$ , where  $a$  is the alloy lattice constant.<sup>19</sup> We therefore estimate  $B_x/B_s$  as

$$B_x/B_s = (a_s/a_x)^4 \approx 1 + 4\varepsilon_{\parallel}^0 \approx 1 - 0.28x, \quad (9)$$

where  $\varepsilon_{\parallel}^0$  is the in-plane strain at  $P=0$ , and depends on the composition  $x$  as  $\varepsilon_{\parallel}^0(x) = -0.07x$  for  $\text{In}_x\text{Ga}_{1-x}\text{As}$  lattice matched to GaAs. Equation (9) implies a reduction in the strained-layer pressure coefficient compared to the free-standing alloy. When we substitute Eq. (9) in the first term of Eq. (8), we find a predicted variation in the direct-band-gap pressure coefficient due to this term of  $10.7 - 3.0x$  meV/kbar. This reduction is not sufficient to account for the experimental data. We shall, in any case, show now how the second term on the right-hand side of (8) is predicted to act in the opposite direction, and increase  $dE_g/dP$ .

The pressure dependence of the axial strain can be estimated using elasticity theory. The elastic energy density  $U$  of a (001)-strained crystal is given by

$$U = \frac{1}{2}C_{11}(\varepsilon_{xx}^2 + \varepsilon_{yy}^2 + \varepsilon_{zz}^2) + C_{12}(\varepsilon_{yy}\varepsilon_{zz} + \varepsilon_{zz}\varepsilon_{xx} + \varepsilon_{xx}\varepsilon_{yy}) + \frac{1}{6}C_{111}(\varepsilon_{xx}^3 + \varepsilon_{yy}^3 + \varepsilon_{zz}^3) + C_{123}\varepsilon_{xx}\varepsilon_{yy}\varepsilon_{zz} + \frac{1}{2}C_{112}(\varepsilon_{xx}^2\varepsilon_{yy} + \varepsilon_{xx}\varepsilon_{yy}^2 + \varepsilon_{yy}^2\varepsilon_{zz} + \varepsilon_{yy}\varepsilon_{zz}^2 + \varepsilon_{zz}^2\varepsilon_{xx} + \varepsilon_{zz}\varepsilon_{xx}^2), \quad (10)$$

where  $C_{11}$  and  $C_{12}$  are the second-order elastic constants, and  $C_{111}$ ,  $C_{123}$ , and  $C_{112}$  are the third-order elastic constants. The pressure along the  $i$ th direction is related to the crystal distortion by

$$P_i = -\frac{\partial U}{\partial \varepsilon_{ii}}. \quad (11)$$

We calculate  $d\varepsilon_{ax}/dP$  by noting that  $\varepsilon_{\parallel}(P)$  is determined by the variation in the lattice constant of the GaAs substrate, while  $\varepsilon_{\perp}(P)$  can then be found from Eqs. (10) and (11) using the previously determined value of  $\varepsilon_{\parallel}(P)$ . We find in second-order elasticity theory that

$$\frac{d\varepsilon_{ax}}{dP} = \frac{1}{3}(B_s^{-1} - B_x^{-1}) \frac{1 + \sigma_x}{1 - \sigma_x}, \quad (12)$$

where  $\sigma_x$  is Poisson's ratio for the alloy. As  $B$  decreases with increasing lattice constant,  $d\varepsilon_{ax}/dP$  is therefore negative, and the net axial strain decreases in second-order elasticity theory. We combine Eqs. (7), (9), and (12) and estimate that

$$\begin{aligned} (\alpha + \ell) \frac{d\varepsilon_{ax}}{dP} &= -\frac{4}{3} \left[ 1 + \frac{\ell}{\alpha} \right] \varepsilon_{\parallel}^0 \frac{1 + \sigma_x}{1 - \sigma_x} \frac{dE_g^0}{dP} \\ &\approx -\frac{10}{3} \varepsilon_{\parallel}^0 \frac{dE_g^0}{dP}, \end{aligned} \quad (13)$$

where we choose as typical values  $\sigma_x = \frac{1}{3}$  and  $\ell/\alpha = \frac{1}{4}$ . When we substitute (9) and (13) in (8), we estimate in second-order elasticity theory, with strain-independent

deformation potentials, that

$$\begin{aligned} \frac{dE_g(x)}{dP} &= (1 + \frac{2}{3}\varepsilon_{\parallel}^0) \frac{dE_g^0}{dP} \\ &= 10.7 - 0.5x \text{ meV/kbar}, \end{aligned} \quad (14)$$

so that the calculated variation in pressure coefficient with composition is significantly smaller than the experimentally determined variation.

We have investigated and find that Eq. (14) is not significantly modified when we include third-order elastic constants or strain-dependent deformation potentials. The full set of third-order elastic constants have been measured for GaAs.<sup>20</sup> We presume that all the elastic constants vary with lattice constant as  $a^4$  and have evaluated numerically  $\varepsilon_{\parallel}(P)$  and  $\varepsilon_{\perp}(P)$  as functions of alloy composition  $x$ . We find that inclusion of the third-order elastic constants approximately halves the pressure dependence of the axial strain, so that  $(\alpha + \ell)d\varepsilon_{ax}/dP \approx -\frac{5}{3}\varepsilon_{\parallel}^0 dE_g^0/dP$  and  $dE_g(x)/dP = 10.7 - 1.7x$  meV/kbar, with the variation still down by over a factor of 3 on experiment.

The hydrostatic deformation potential  $\alpha$  describes the relative shift of the conduction-band-minimum energy with respect to the average of the valence-band energies at the  $\Gamma$  point. We can allow for its strain dependence by introducing higher-order deformation potentials so that the average band gap  $E_g$  varies with hydrostatic and axial strain,  $\varepsilon_{\text{vol}}$  and  $\varepsilon_{\text{ax}}$ , as

$$E_g = E_g^0 + \alpha\varepsilon_{\text{vol}} + \alpha_{\text{ax}}\varepsilon_{\text{ax}}^2 + \alpha_v\varepsilon_{\text{vol}}^2, \quad (15)$$

with the band-gap pressure dependence then being given by

$$\frac{dE_g}{dP} = (a + 2a_v \epsilon_{vol}) \frac{d\epsilon_{vol}}{dP} + 2a_{ax} \epsilon_{ax} \frac{d\epsilon_{ax}}{dP}. \quad (16)$$

Experiments and calculations indicate that  $a_v \gtrsim 0$  in GaAs,<sup>14</sup> so that the second-order volume deformation potential will tend if anything to increase the measured pressure dependence of the band gap, as  $\epsilon_{vol} d\epsilon_{vol}/dP > 0$ . We do not know of any published measurement or calculation of  $a_{ax}$  for GaAs, but note that the deformation potentials in Eq. (15) have been calculated for strained GaSb by Qteish and Needs using self-consistent local-density calculations.<sup>21</sup> They find  $a_{ax} = -8.69$  eV in GaSb. The negative sign of  $a_{ax}$  arises from a strain-induced mixing between the lowest conduction band and higher-lying conduction states; as this mixing occurs in all III-V compound semiconductors, we expect that  $a_{ax}$  is also negative in  $\text{In}_x\text{Ga}_{1-x}\text{As}$ , so that  $a_{ax}\epsilon_{ax} d\epsilon_{ax}/dP > 0$  in second- and third-order elasticity theory, again leading to a small enhancement of the pressure dependence of the alloy band gap.

We next consider the strain dependence of the axial deformation potential  $\ell$ . This can only contribute to a reduced measured pressure coefficient if the magnitude of  $\ell$  increases very rapidly with increasing hydrostatic pressure, at an estimated rate of 1%/kbar. We consider that such a pressure dependence is most unlikely, as it would imply  $\ell$  increasing by 50% for a 3% change in volume, while  $\ell$  is calculated to have only a weak strain dependence in GaSb,<sup>21</sup> and shows little variation between different III-V compound semiconductors.<sup>3</sup> We further note that any corrections to the deformation potentials will vary quadratically with axial strain  $\epsilon_{ax}$ , and so will have difficulty in explaining the observed linear variation of the pressure coefficient with  $\epsilon_{ax}$ .

Our calculations above indicate that direct interpolation and estimation of bulk crystal properties cannot account for the measured pressure dependence of the band gap as a function of alloy composition. We must therefore seek other explanations related to deviations from perfect-crystalline properties. We do not believe that the photoluminescence is related to extrinsic defects, as the spectra are characteristic of quantum-well free-exciton emissions, and also because we measure small Stokes shifts (1–2 meV) in similar single-quantum-well samples. We therefore consider the possibility and effects of compositional and well-width fluctuations in the alloy layers. The photoluminescence from a quantum well is associated with those regions where the band gap is smallest. These will tend to be regions where the alloy composition is higher than average, and as the bulk modulus  $B_x$  decreases with  $x$ , the ratio  $B_x/B_s$  will also tend to be reduced in such regions, implying from Eq. (8) a reduced pressure coefficient of the band gap. Fluctuations will also introduce nonuniform strains into the structure, leading to the possibility of local regions where  $d\epsilon_{ax}/dP > 0$ , and again the possibility of a reduced pres-

sure dependence.

It is difficult to quantify these effects because the measured pressure dependence of the band gap depends on both the alloy deformation potentials and on  $d\epsilon_{ax}/dP$  [see Eq. (6)]. It is thus impossible to deduce the alloy hydrostatic deformation potential,  $\alpha$ , without a knowledge of  $d\epsilon_{ax}/dP$ , or vice versa. Our PL data suggest that  $\alpha$  and/or  $d\epsilon_{ax}/dP$  is (are) varying anomalously with alloy composition  $x$ . We can estimate limits on the possible anomalous variation of either quantity by interpolating the other in a reasonable manner. We first assume that the pressure dependence of the axial strain is well described by third-order elasticity theory, from which we estimated

$$\begin{aligned} \frac{d\epsilon_{ax}}{dP} &\approx \frac{1}{3B_s} \left[ 1 - \frac{B_s}{B_x} \right] \\ &\approx -0.09x/B_s. \end{aligned}$$

If we set  $\ell=0$  in Eq. (6) and take the bulk modulus of GaAs as 747 kbar,<sup>22</sup> we then estimate the bulk hydrostatic deformation potential  $\alpha$  to vary with alloy composition  $x$  as  $\alpha(x) = -(7.99 - 3.76x)$  eV for small  $x$ .

Alternatively, we can assume, as earlier, that the pressure dependence of the unstrained alloy band gap is approximately independent of alloy composition,  $dE_g^0(x)/dP = 10.7$  meV/kbar, in which case we calculate from Eq. (8) that  $(\alpha + \ell)d\epsilon_{ax}/dP = -3.0x$  meV/kbar, and taking 10 eV as a typical value of  $\alpha + \ell$  then gives  $d\epsilon_{ax}/dP \approx -0.05\epsilon_{||}^0$  kbar<sup>-1</sup>. This corresponds to a doubling of the built-in axial strain  $\epsilon_{ax}$  for an applied hydrostatic pressure of 40 kbar in some parts of the strained layer.

These estimates show that interpretation of the experimental data in this manner requires the introduction of a surprisingly large variation with alloy composition of either the band-gap deformation potential  $\alpha$  or the built-in axial strain  $\epsilon_{ax}$ . It is clear that further studies are appropriate to quantify the degree of disorder and well-width fluctuations in strained quantum wells and to determine what effects are dominating in our experiments.

#### IV. CONCLUSIONS

The pressure coefficient of the photoluminescence of various quantum wells implies that the pressure coefficient of bulk strained pseudomorphic  $\text{In}_x\text{Ga}_{1-x}\text{As}$  is  $10.7 - 6.0x$  meV/kbar, in contrast to the values of 10.7 meV/kbar in GaAs and of 10.9 meV/kbar measured in unstrained  $\text{In}_{0.53}\text{Ga}_{0.47}\text{As}$ , and the value of  $10.7 - 1.7x$  meV/kbar predicted by third-order elasticity theory. The variation in band-gap deformation potential deduced from the pressure coefficient could be as large as  $-(7.99 - 3.76x)$  eV for small  $x$ . This result is not understood, but may be related to disorder-induced effects as-

sociated with the alloy nature of the  $\text{In}_x\text{Ga}_{1-x}\text{As}$  layers. Further work should be undertaken to identify positively the origin of this effect, which must be taken into account in any study of the electronic structure of pseudomorphic  $\text{In}_x\text{Ga}_{1-x}\text{As}/\text{GaAs}$  heterostructures.

#### ACKNOWLEDGMENTS

We are grateful to the United Kingdom Science and Engineering Research Council for financial support, and to A. Qteish and R. J. Needs for making their results available prior to publication.

\*Also at the Department of Physics.

- <sup>1</sup>P. B. Kirby, J. A. Constable, and R. S. Smith, *Phys. Rev. B* **40**, 3013 (1989).
- <sup>2</sup>L. E. Eng, T. R. Chen, S. Sanders, Y. Z. Zhuang, B. Zhao, and A. Yanv, *Appl. Phys. Lett.* **55**, 1378 (1989).
- <sup>3</sup>E. P. O'Reilly, *Semicond. Sci. Technol.* **4**, 121 (1989).
- <sup>4</sup>D. J. Wolford, T. F. Kuech, J. A. Bradley, M. A. Gell, D. Nimmo, and M. Jaros, *J. Vac. Sci. Technol. B* **4**, 1043 (1986).
- <sup>5</sup>L. Wang, H. Hou, Z. Zhou, R. Tang, Z. Lu, Y. Wang, and Q. Huang, *Chin. Phys. Lett.* **6**, 76 (1989).
- <sup>6</sup>A. D. Prins, J. D. Lambkin, K. P. Homewood, M. T. Emeny, and C. R. Whitehouse, *High Press. Res.* **3**, 51 (1990).
- <sup>7</sup>L. K. Howard, K. P. Homewood, M. T. Emeny, and C. R. Whitehouse (unpublished).
- <sup>8</sup>See, for example, J. W. Matthews and A. E. Blakeslee, *J. Cryst. Growth* **29**, 273 (1975).
- <sup>9</sup>R. H. Dixon and P. J. Goodhew, *J. Appl. Phys.* (to be published).
- <sup>10</sup>A. D. Prins, I. L. Spain, and D. J. Dunstan, *Semicond. Sci. Technol.* **4**, 237 (1989).
- <sup>11</sup>W. Paul and D. M. Warschauer, *Solids at High Pressure* (McGraw-Hill, New York, 1963), Chap. 8, p. 226.
- <sup>12</sup>J. D. Lambkin, D. J. Dunstan, E. P. O'Reilly, and B. R. Butler, *J. Cryst. Growth* **93**, 323 (1988).
- <sup>13</sup>H. Muller, R. Trommer, and M. Cardona, *Phys. Rev. B* **21**, 4879 (1989).
- <sup>14</sup>A. R. Goni, K. Stroessner, K. Syassen, and M. Cardona, *Phys. Rev. B* **36**, 1581 (1987).
- <sup>15</sup>P. Lefebvre, B. Gil, and H. Mathieu, *Phys. Rev. B* **35**, 5630 (1987).
- <sup>16</sup>C. G. Van de Walle, *Phys. Rev. B* **39**, 1871 (1989).
- <sup>17</sup>Y. F. Tsay, S. S. Mitra, and B. Bendow, *Phys. Rev. B* **10**, 1 (1974).
- <sup>18</sup>J. D. Lambkin and D. J. Dunstan, *Solid State Commun.* **67**, 627 (1988).
- <sup>19</sup>A. D. Prins and D. J. Dunstan, *Philos. Mag. Lett. B* **58**, 37 (1988).
- <sup>20</sup>J. R. Drabble and A. J. Brammer, *Solid State Commun.* **4**, 467 (1966); H. J. McSkimmin and P. Andreatch, *J. Appl. Phys.* **38**, 2610 (1967).
- <sup>21</sup>A. Qteish and R. J. Needs, *Phys. Rev. B* **42**, 3044 (1990).
- <sup>22</sup>H. J. McSkimmin, A. Jayaraman, and P. Andreatch, *J. Appl. Phys.* **38**, 2362 (1967).